Available online at www.sciencedirect.com
SCIENCE DIRECT
Chemical Physics Letters 417 (2006) 230–234
CHEMICAL PHYSICS LETTERS
www.elsevier.com/locate/cplett

Surface-enhanced Raman scattering of 4-mercaptopyridine on thin films of nanoscale Pd cubes, boxes, and cages

Joseph M. McLellan, Yujie Xiong, Min Hu, Younan Xia *

Department of Chemistry, University of Washington, Seattle, WA 98195-1700, USA

Received 23 September 2005
Available online 27 October 2005

Abstract

We have synthesized a variety of Pd nanoparticles of 8–50 nm in size including solid cubes, hollow boxes, and porous cages. Using 4-mercaptopyridine (4MP) as a probe molecule, we have characterized thin films for surface-enhanced Raman scattering (SERS) activity, and have found a significant level of enhancement (with factors ranging from 170 for 8-nm cubes to 1.3×10^4 for boxes). For the cubes and boxes, we observed a trend of stronger enhancement with more red-shifted SPR bands. We evaluated the sensitivity of this approach, and also used SERS to monitor monolayer formation on these particles.

1. Introduction

Interest in surface-enhanced Raman scattering (SERS) has truly blossomed over the last decade and a half. Most of the efforts have focused on the use of coinage metal substrates (Ag, Au, and Cu) due to their extremely high enhancement factors, which have even enabled single molecule detection [1]. It has been widely accepted that there are two primary enhancement mechanisms in SERS: one being electromagnetic (EM) enhancement that arises from the extremely high local fields due to surface plasmon resonance (SPR) and the other being chemical enhancement due to resonance Raman-like interaction between the substrate and the adsorbate [2]. For noble metals, enhancement of SERS signals tends to be primarily caused by the EM effect. In principle, the position of an SPR band for a metal nanoparticle can be controlled by varying the composition, size, and shape [3]. The SPR bands of the aforementioned coinage metal nanoparticles are typically located in the visible to near-infrared (NIR) regions, and thus have been the substrates of choice for conventional Raman systems, which utilize visible to NIR lasers. However, the wide application of other noble metals such as Pd, Pt, and Rh in catalysis, make the extension of SERS to these metals attractive.

To this end, several approaches have been developed. The first of these can generally be described as a 'borrowing' technique where a less SERS-active material is deposited on a SERS-active substrate and 'borrows' from the strong local field generated in the SERS-active material. This approach has been demonstrated in a variety of ways ranging from thin metallic films (3–10 atomic layers) deposited on roughened electrodes [4–6] to core–shell [7–9] and hybrid [10,11] bimetallic nanoparticles. For all of these demonstrations, the SERS enhancement rapidly decreased with increasing shell or overlayer thickness. Other approaches have focused on the use of monometallic nanoparticles by synthesizing Pt [9,12,13], Pd [13,14] and Rh [15] sols, and then using aggregated films of these particles for SERS. However, in all of these cases the particles were less than 20 nm and showed no SPR band in the visible or NIR regions. Since these metals generally have a small imaginary part in their dielectric constants, their SPR bands are typically located in the UV region. Tian and co-workers [16] recently demonstrated the application of UV-SERS, and showed modest enhancement from roughened Rh and Ru surfaces as compared to Ag particles when

* Corresponding author. Fax: +1 206 685 8665.
E-mail address: xia@chem.washington.edu (Y. Xia).

0009-2614/$ - see front matter © 2005 Elsevier B.V. All rights reserved.
doi:10.1016/j.cplett.2005.10.028

325 nm irradiation was used. Most recently we have successfully synthesized Pd nanoparticles with edge lengths of 25 nm and above and further processed them into hollow structures. All these Pd nanoparticles exhibited SPR bands in the visible region. Here, we demonstrate the SERS activities of thin films consisting of these Pd nanoparticles, and compare their activities as a function of size, solidity (solid versus hollow), and thus the positions of SPR bands.

2. Experimental

2.1. Preparation of Pd nanoparticles

The procedures for synthesizing Pd nanocubes, nanoboxes, and nanocages have already been published [17,18]. Briefly, these nanoparticles were synthesized using a polyol method in which Na_2PdCl_4 was reduced by ethylene glycol (EG) in the presence of poly(vinyl pyrrolidone) (PVP). When the same concentration of precursor was used, the size of the cubes could be controlled by adjusting the density of seeds formed in the nucleation step. The synthesis of nanoboxes and nanocages was similar, except water was added to increase the solubility of oxygen and thus oxidative corrosion. Cubes were formed initially, but these could be transformed into boxes and further into cages with time. Following synthesis, the particles were washed with acetone and then by ethanol several times to remove EG and excess PVP, and finally redispersed in deionized water. Samples were characterized by UV–vis spectroscopy (HP 8452A diode array spectrometer), and transmission electron microscopy (TEM). TEM samples were prepared by drying aqueous suspensions of the particles on carbon coated TEM grids under ambient conditions. TEM images were taken on a Phillips 420 transmission electron microscope operated at 120 kV.

2.2. Raman spectroscopic measurement

SERS substrates were prepared by drop-casting 5 μL of the aqueous sol on a Si wafer and allowed to completely dry under vacuum. The dry films were immersed in a 4 mM aqueous solution of 4-mercaptopryidine (4MP) for 1 h. The samples were then taken out, rinsed with deionized water to remove any unadsorbed 4MP molecules, and dried with a stream of air. For the nanoboxes, two series of samples were prepared: one with solutions of 4MP that ranged from 4 mM to 4 pM and another where films were immersed in a 4 mM solution for different periods of time. Raman spectra were obtained using a Renishaw inVia Raman spectrometer (HPNIR785) attached to a Leica DM IRBE optical microscope. A spot size of ~1.6 μm in diameter and 785-nm laser excitation from a diode laser at a power of 3 mW at the sample surface were used to irradiate the samples. The Raman scattering signals were collected on a thermoelectrically cooled (−60 °C) CCD detector.

3. Results and discussion

3.1. Comparison of SERS activity

Our group has recently demonstrated shape-controlled synthesis for a number of noble metals (e.g., Ag, Pt, Pd, and Rh) with an emphasis on how the positions of SPR bands are determined by the size, shape, and composition of the particles [11,17–21]. One particularly interesting example is Pd, for which we have synthesized solid cubes [17] with average edge lengths ranging from 8 to 50 nm, as well as hollow boxes and cages [18] with edge lengths of ~50 nm. Fig. 1 shows UV–vis absorption spectra and corresponding TEM images for the Pd nanoparticles that were used for SERS measurements. Nanocubes with edge

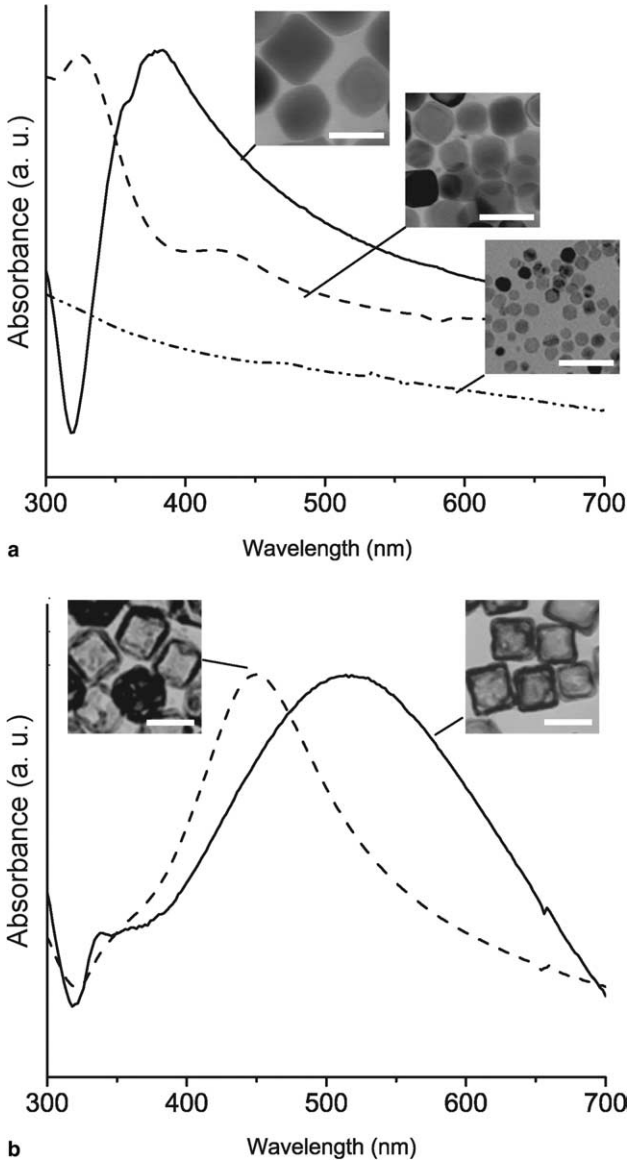

Fig. 1. Extinction spectra and corresponding TEM images of Pd nanoparticles. (a) From top to bottom 50-nm (solid line), 25-nm (dashed), and-8 nm cubes (doted). (b) Pd nanoboxes (left image; dashed line) and nanocages (right image; solid line). All scale bars correspond to 50 nm.

lengths of 8, 25, and 50 nm showed SPR bands peaked at 225, 330, and 390 nm, respectively (Fig. 1a). Note that for the 8-nm cubes, only a 'tail' can be seen extending from the UV to the visible region. By processing 48-nm cubes into hollow structures the SPR bands could be further red-shifted. Fig. 1b shows typical spectra and TEM of such Pd nanoboxes and nanocages. The positions of all these SPR bands were consistent with the results of discrete dipole approximation (DDA) calculations [17,18].

The highest EM field enhancement arises when the irradiation wavelength is resonant with the SPR maximum [22,23]. For SERS measurements we used a 785 nm laser, so one could expect to see enhanced SERS activity for those particles with more red-shifted SPR bands. Fig. 2 compares the SERS spectra of 4MP on thin films of 8-, 25-, and 50-nm Pd cubes. We chose 4MP as a probe molecule because: (i) it has been well established in the literature [24]; (ii) it will form a monolayer on the surface of Pd nanoparticle making the estimate of surface coverage more convenient [25]; (iii) it has a large scattering cross-section [26]. We also investigated the activity of Pd hollow nanoparticles that have even more red-shifted SPR bands. Fig. 3 shows SERS spectra obtained from films of 50-nm nanoboxes and nanocages. We found that the nanoboxes gave the strongest enhancement among all the samples. The results unambiguously demonstrate the activity of Pd for SERS. For Pd nanocubes and nanoboxes, the SERS intensity was greatly enhanced as the SPR band of these particles was red-shifted. However, the weaker activity of the nanocages is hard to understand, because the cages have the most red-shifted SPR band and they are expected to have the strongest enhancement. A plausible explanation is that a change in the structure of these particles not only effects the position of the SPR band, but also the contributions of scattering and absorption to the

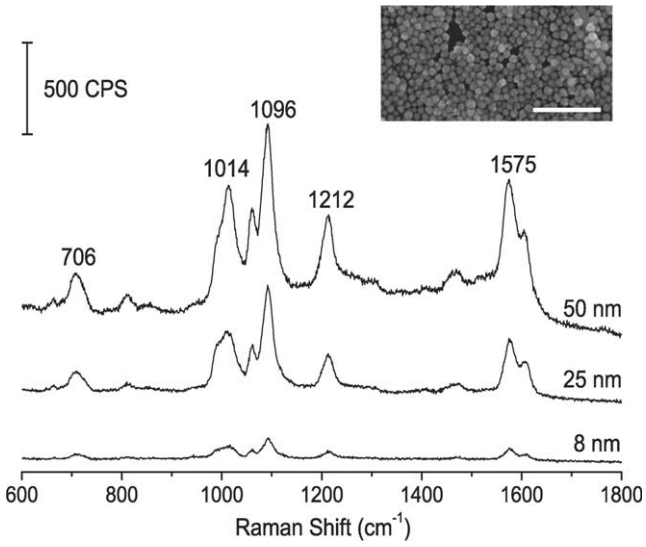

Fig. 2. SERS spectra of 4-mercaptopyridine (4MP) adsorbed on films of Pd nanocubes with 50, 25, and 8 nm edge lengths. The inset shows a typical SEM image of the thin film containing 50-nm Pd cubes, where the scale bar corresponds to 500 nm.

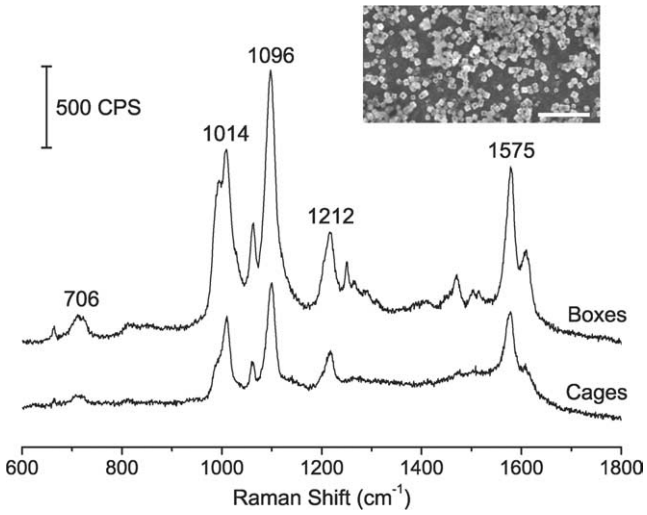

Fig. 3. SERS spectra of 4-mercaptopyridine (4MP) adsorbed on thin films of Pd nanoboxes and nanocages. The inset shows a typical SEM image of the film containing 50-nm nanoboxes that was used for SERS measurements. The scale bar corresponds to 500 nm.

extinction spectra, as well as overall optical cross-section [18]. For example, the cages have a thinner wall relative to the boxes, and this difference in structure could have a significant effect on the overall EM enhancement. This observation suggests that while the position of the SPR band relative to the excitation wavelength is important for SERS, there may be other significant contributions to the enhancement mechanism such as aggregation effects. It also highlights one of the challenges that have plagued SERS since its infancy, that is, the inconsistent substrate performance.

To evaluate the limit of detection for this system, we prepared solutions ranging from 4 mM to 4 pM, immersed nanobox films in them for 1 h, and then took SERS signals from the films. The results of this experiment are shown in Fig. 4, together with a typical SEM image of the films. For the 4 pM sample no identifiable peaks were observed, however recognizable to high-quality spectra were obtained for all other samples. The inset corresponds to a 10× magnification of the 1030–1130 cm^{-1} region for the sample prepared from 1 nM 4MP. Even though the signal-to-noise ratio of this spectrum was extremely poor, it still seems to be possible to detect the adsorbed 4MP molecules at this concentration level, and at higher quality spectra might be obtainable by optimizing the acquisition time and the number of accumulations.

The high sensitivity of SERS could also be used to investigate the formation of 4MP monolayer on the surface of Pd nanoparticles. Monolayer formation is typically monitored using a combination of techniques such as contact angle or elipsometry measurements and X-ray photoelectron spectroscopy; results are typically plotted as a function of immersion time. We demonstrate here that SERS can also be used in the same way to monitor the formation kinetics. As shown in Fig. 5, we plotted the integrated intensity of the 1096 cm^{-1} band for 4MP adsorbed on Pd

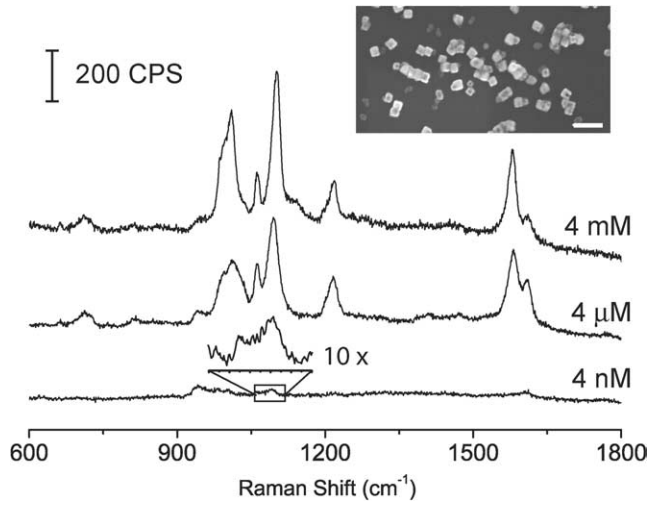

Fig. 4. SERS spectra from thin films of Pd nanoboxes that had been functionalized with aqueous 4-mercaptopyridine (4MP) solutions that ranged from 4×10^{-3} to 4×10^{-9} M. A distinct peek at 1096 cm^{-1} could still be observed for the 4×10^{-9} M sample by magnifying the signals in the 1030–1130 cm^{-1} region (see the inset). The inset at the top shows a typical SEM image of the nanobox film that was functionalized with a 4 mM solution. The scale bar corresponds to 200 nm.

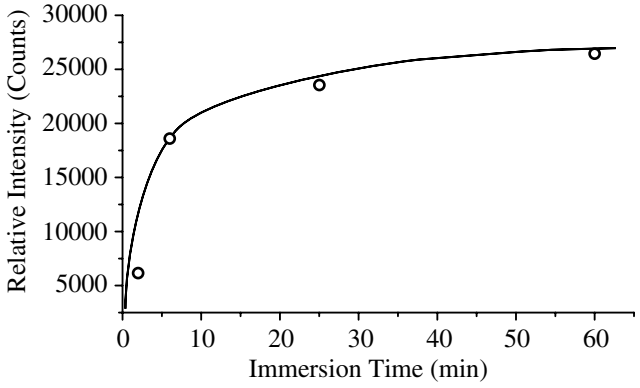

Fig. 5. Plot of the relative intensity of the 1096 cm^{-1} band in the SERS spectra of 4-mercaptopyridine (4MP) adsorbed on Pd nanoboxes as a function of the immersion time. A 4-mM aqueous solution of 4MP was used.

nanoboxes as a function of immersion time. The shape of the curve is consistent with a typical Langmuir adsorption process. The major advantage of using SERS to monitor the kinetics is that unlike elipsometry or contact angle measurements, one obtains structural and compositional data too. In addition, a stronger enhancement might enable monitoring of molecular adsorption on individual particles, a task not readily accomplished using other techniques.

3.2. Estimate of the surface enhancement factor

To quantify the results, we calculated surface enhancement factors, G, for the samples shown in Figs. 1 and 2 using methods described by Tian and coworkers [26]

$$G=\frac{I_{surf}/N_{surf}}{I_{bulk}/N_{bulk}}. \quad (1)$$

In Eq. (1), I_{surf} and I_{bulk} are the integrated intensities of the same ν_{1a} bands for the adsorbed 4MP and unadsorbed 4MP molecules respectively, and similarly the N_{surf} and N_{bulk} are the number of adsorbed and unadsorbed 4MP molecules contributing to the signal. For the bulk (unadsorbed) 4MP we used a 0.3 M aqueous solution. In order to determine the number of molecules that contributed to the I_{bulk} signal we had to determine the confocal depth profile of our microscope [26]. For the optical configuration and microscope employed in this work, the confocal depth was 13 μm. We used a spot size of 1.6 μm giving a focal volume of 0.1 pL, and thus N_{bulk}, for a 0.3 M solution, would be 2×10^{10} 4MP molecules. We estimated the number of 4MP molecules sampled (N_{surf}), in the case of the 50-nm cubes, to be 1.9×10^{9}. Using the 1096 cm^{-1} band, I_{surf} and I_{bulk} were 1.7×10^{4} and 180, respectively. From these numbers, we calculated an enhancement factor of 9.3×10^{3} for the film of 50-nm cubes, and 2.2×10^{3} and 170 for the 25- and 8-nm cubes, respectively. For the nanoboxes, we calculated an enhancement factor of 1.3×10^{4}, while we found an enhancement factor of only 7.5×10^{3} for the nanocages. The enhancement factors given here are for typical samples, and it should be noted that we did often observe a marked variation in SERS enhancement from sample to sample, even when prepared under identical conditions. This observation is a good indication that the way in which the particles aggregate upon drying may play a critical role in the enhancement mechanism, as has been seen with Ag and Au nanoparticles [23,24,27–30].

4. Summary

A variety of Pd cubic nanoparticles have been synthesized using the polyol method, and characterized by UV–vis spectroscopy and TEM. Thin films of each of type of particles were prepared, functionalized with monolayers of 4MP, and then used for SERS measurements with a confocal Raman microscope. We found that (i) these particles exhibited extraordinary high SERS activity, as compared to previous demonstrations of SERS on Pd nanoparticles [14] and (ii) there was a strong correlation between the SERS intensity and the size or solidity of the particles. The activity is most likely due to a combination of the enhancement arising from the significant EM field enhancement due to SPR and aggregation effects, as indicated by the correlation of SERS activity to SPR position and variation of the SERS intensity from samples prepared under identical conditions, respectively. For the nanocubes and nanoboxes a trend of higher SERS activity with red-shifted SPR peak was observed. However, in the case of nanocages, which had the most red-shifted SPR band, we found a surface enhancement factor that was almost half that of the nanoboxes (1.3×10^{4} versus 7.5×10^{3}). We are

currently working to better understand this result as it appears to be contrary to predictions based on DDA calculations for Au nanocages [31], and thus could shed light on the SERS enhancement mechanism for Pd nanoparticles. We also looked at films of Pd nanoboxes that were functionalized with very dilute 4MP solutions (4 nM), and without optimization, we were able to obtain recognizable spectra. Finally, we also demonstrate how SERS could be used to follow the formation kinetics of monolayers on Pd nanoparticles.

Acknowledgments

This work was supported in part by the MLSC Program at the UW and a fellowship from the David and Lucile Packard Foundation. Y.X. is an Alfred P. Sloan Research Fellow and a Camille Dreyfus Teacher Scholar. M.H. is an INEST Postdoctoral Fellow supported by Phillip Morris USA. Instrumentation was provided by the Nanotech User Facility (NUTF), a member of the National Nanotechnology Infrastructure Network (NNIN) supported by NSF.

References

[1] S.M. Nie, S.R. Emory, Science 275 (1997) 1102.
[2] Z.Q. Tian, B. Ren, D.Y. Wu, J. Phys. Chem. B. 106 (2002) 9463.
[3] A.J. Hayes, C.L. Haynes, A.D. McFarland, G.C. Schatz, R.P. Van Duyne, S. Zou, MRS Bull. 30 (2005) 368.
[4] M. Fleischmann, Z.Q. Tian, L.J. Li, J. Electroanal. Chem. 217 (1987) 397.
[5] Q. Feng, T.M. Cotton, J. Phys. Chem. 90 (1986) 983.
[6] Y. Zhang, X. Gao, M.J. Weaver, J. Phys. Chem. 97 (1993) 8656.
[7] J.W. Hu, Y. Zhang, J.F. Li, Z. Liu, B. Ren, S.G. Sun, Z.Q. Tian, T. Lian, Chem. Phys. Lett. 408 (2005) 354.
[8] B. Zhang, J.F. Li, Q.L. Zhong, B. Ren, Z.Q. Tian, S.Z. Zou, Langmuir 21 (2005) 7449.
[9] Z.Q. Tian, Z.L. Yang, B. Ren, J.F. Li, Y. Zhang, X.F. Lin, J.W. Hu, D.Y. Wu, Faraday Discuss. 132 (13) (2005), preprint.
[10] B. Pergolese, A. Bigotto, G. Muniz-Miranda, G. Sbrana, Appl. Spectrosc. 591 (2005) 194.
[11] J. Chen, B. Wiley, J. McLellan, Y. Xiong, Z.Y. Li, Y. Xia, Nano Lett. 5 (2005) 2058.
[12] N.H. Kim, K. Kim, Chem. Phys. Lett. 393 (2004) 478.
[13] R. Gömez, J.M. Pérez, J. Solla-Gullón, V. Montiel, A. Aldaz, J. Phys. Chem. B 108 (2004) 9943.
[14] I. Srnová, B. Vlčková, V. Baumruk, J. Mol. Stuct. 410–411 (1997) 201.
[15] W.L. Parker, R.M. Hexter, Chem. Phys. Lett. 107 (1984) 96.
[16] B. Ren, X.F. Lin, Z.L. Yang, G.K. Liu, R.F. Aroca, B.W. Mao, Z.Q. Tian, J. Am. Chem. Soc. 125 (2003) 9598.
[17] Y. Xiong, J. Chen, B. Wiley, Y. Xia, Y. Yin, Z.Y. Li, Nano Lett. 5 (2005) 1237.
[18] Y. Xiong, B. Wiley, J. Chen, Z.Y. Li, Y. Yin, Y. Xia, Angew. Chem. Int. Ed. (2005) (in press).
[19] N. Zettsu, J.M. McLellan, B. Wiley, Y. Yin, Z.Y. Li, Y. Xia, Angew. Chem. Int. Ed. (under review).
[20] Y. Sun, Y. Xia, Analyst 128 (2003) 686.
[21] B. Wiley, Y. Sun, J. Chen, H. Cang, Z.Y. Li, X. Li, Y. Xia, MRS Bulletin 30 (2005) 356.
[22] N. Halas, MRS Bull. 30 (2005) 362.
[23] A.M. Scwartberg, C.D. Grant, A. Wolcott, C.E. Talley, T.R. Huser, R. Bogomolni, J.Z. Zhang, J. Phys. Chem. B 108 (2004) 19191.
[24] Z. Wang, S. Pan, T.D. Krauss, H. Du, L.J. Rothberg, Proc. Natl. Acad. Sci. USA 100 (2003) 8638.
[25] S. Chen, K. Huang, J.A. Stearns, Chem. Mater. 12 (2000) 540.
[26] W.B. Cai, B. Ren, X.Q. Li, C.X. She, F.M. Liu, X.W. Cai, Z.Q. Tian, Surf. Sci. 406 (1998) 9.
[27] P.M. Tessier, O.D. Velev, A.T. Kalambur, J.F. Rabolt, A.M. Lenhoff, E.W. Kaler, J. Am. Chem. Soc. 122 (2000) 9554.
[28] D.M. Kuncicky, S.D. Christesen, O.D. Velev, Appl. Spectrosc. 59 (2005) 401.
[29] A.R. Tao, P. Yang, J. Phys. Chem. B 109 (2005) 15687.
[30] A. Tao, F. Kim, C. Hess, J. Goldberger, R. He, Y. Sun, Y. Xia, P. Yang, Nano. Lett. 3 (2003) 1229.
[31] E. Hao, S. Li, R.C. Bailey, S. Zou, G.C. Schatz, J.T. Hupp, J. Phys. Chem. B 108 (2004) 1224.